# Direct observation of nanoparticle-ubiquitin corona formation

Feng Ding[1], Slaven Radic[1], Ran Chen[1], Pengyu Chen[1], Nicholas K. Geitner[1], Jared M. Brow[2] and Pu Chun Ke[1]

[1]Department of Physics and Astronomy, Clemson University, Clemson, South Carolina 29634, United States; [2]Department of Pharmacology and Toxicology, Brody School of Medicine, East Carolina University, Greenville, NC 27858 (USA)

E-mail: fding@clemson.edu; pcke11@clemson.edu

## ABSTRACT

Upon entering physiological environments, nanoparticles readily assume the form of a nanoparticle-protein corona that dictates their biological identity. Understanding the structure and dynamics of nanoparticle-protein corona is essential for predicting the fate, transport, and toxicity of nanomaterials in living systems and for enabling the vast applications of nanomedicine. We combined multiscale molecular dynamics simulations and complementary experiments to characterize the silver nanoparticle-ubiquitin corona formation. Specifically, ubiquitins competed with citrates for the nanoparticle surface and bound to the particle in a specific manner. The specific binding between a silver nanoparticle and ubiquitin is governed by electrostatic interactions as observed in previous experiments. Under a high protein/nanoparticle stoichiometry, ubiquitins formed a multi-layer corona on the particle surface. The binding exhibited a stretched-exponential behavior, suggesting a rich protein-nanoparticle binding kinetics. Furthermore, the binding destabilized the α-helices while increasing the β-sheets of the proteins. Our results revealed the structural and dynamic complexities of nanoparticle-protein corona formation and shed light on the origin of nanotoxicity.

**Keywords**: nanotechnology, nanoparticle-protein corona, multiscale molecular dynamics, protein conformational change, nanotoxicity

## INTRODUCTION

Nanomaterials have been increasingly applied in consumer products due to their unique physical and chemical properties. The increasing application of nanomaterials in daily life inevitably leads to their accumulation in the environment[1] and subsequent entry into biological systems, causing bio-safety concerns related to nanotechnology[2]. Nanoparticles have also been found useful in disease diagnostics, drug and gene delivery, and therapeutics. Therefore, the safety issue of nanotechnology is pressing, and the study of nanotoxicology has attracted much research interest recently[3]. The benefits of understanding the interactions between nanoparticles and biological systems extend from fundamental physical sciences to nanomedicine, nanotoxicology, nanoecotoxicology, consumer usages, and the public's perception of nanotechnology.

Upon entering biological systems such as the bloodstream, a nanoparticle forms molecular complexes with encountered proteins, termed as the protein corona[4]. Protein corona shields the surface of the exogenous nanoparticle and subsequently determines the biological properties of the nanoparticle core. Recently, protein corona has also been found to screen functionalized molecules conjugated to nanoparticles, and subsequently cause the loss of designed function. On the other hand, interactions with nanoparticles can also alter the structure, dynamics, and function of the bound proteins, which could further impact recognition of the proteins by membrane receptors and the immune system. Previous experimental studies have provided much insight, such as the existence and size of the protein corona[5], and protein composition on the nanoparticle surface[6]. However, due to limitations in instrument resolution, the molecular detail of protein-nanoparticle interaction remains poorly understood. Computational modeling, in contrast, provides a useful approach to bridge the gap between experimental observation and the molecular systems of interest. Here we performed both computational and experimental characterizations of protein corona formation between a silver nanoparticle (AgNP) and ubiquitin protein. Silver nanoparticles are widely used in commercial products for their antibacterial and antifungal properties, while ubiquitin is ubiquitously expressed in all eukaryotic cells regulating protein distribution and recycling. The system of AgNP and ubiquitin is therefore deemed most representative for studying nanoparticle-protein interaction and corona formation.

Two major challenges arise in computational modeling of protein corona. First is the large system size — where an abundance of proteins interacts with nanometer-sized nanoparticles, second is the long timescales associated with protein corona formation. Traditional molecular dynamics approaches can accurately describe the molecular system of nanoparticles and proteins[7-10], but are not able to reach the relevant time and length scales needed for depicting large systems till equilibration[11,12]. In comparison, coarse-grained simulations[13] can be used to study large molecular

systems and reach long time scales by using a simplified forcefield[14]. These coarse-grained simulations have been applied to study the general aspects of NP-protein interactions[13,15-18], but have limited predictive power for studying NP interactions with specific proteins. To overcome this barrier, we adopted a multiscale modeling approach[19], which coherently blended atomistic and coarse-grained simulations[20,21]. All-atom simulations were first performed to investigate the possible binding modes between an individual ubiquitin and an AgNP, and the knowledge of AgNP-ubiquitin binding was then incorporated into the construction of a coarse-grained model. With the coarse-grained simulations, we were able to extensively characterize the structure and dynamics of AgNP interacting with multiple ubiquitin molecules (up to 50). The dynamics of both atomistic and coarse-grained models were sampled by discrete molecular dynamics (DMD), an efficient sampling method for underpinning protein dynamics.

## RESULTS & DISCUSSION

Our transmission electron microscopy and UV-vis absorbance measurements confirmed the binding of ubiquitin and citrate-coated AgNP (Figs. 1a and b). Our dynamic light scattering measurement (data not shown) also corroborated their effective binding. Next, we performed multiscale simulations to characterize the corona formation.

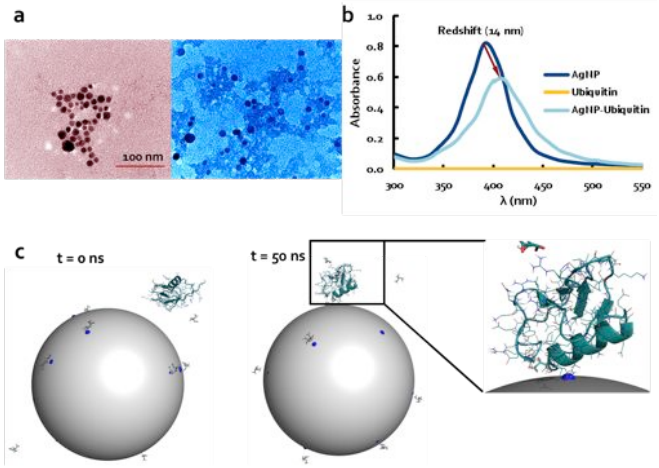


**Figure 1. Interaction between a single ubiquitin and a citrate-coated AgNP.** (a) TEM images of AgNPs (left panel) and AgNP-ubiquitin coronas (right panel). (b) UV-vis absorbance of AgNP, ubiquitin, and AgNP-ubiquitin. (c) Initial (t = 0 ns) and final (t = 50 ns) structure of the ubiquitin-citrate-AgNP complex system. The gray sphere represents the nanoparticle, and the charged atoms on the AgNP surface are shown as blue spheres. Zoom-in view of the final structure indicates the binding between the ubiquitin and a charged AgNP surface atom.

We first performed atomistic simulations of a molecular system comprised of one ubiquitin molecule and one citrate-coated AgNP. The simulations were performed with implicit solvent, and the inter-atomic interactions were modeled by a physical force field adapted from Medusa[22], which include van der Waals, solvation, electrostatic, and hydrogen bond potentials. The coarse-grained silver atoms of the AgNP were assigned as hydrophobic with a small fraction being positively charged to account for the nanoparticle surface charges. During simulations, we kept the center of the AgNP static, while allowing the ubiquitin and the citrates to move freely in the simulation box and surface silver atoms mobile on the nanoparticle surface.

To evaluate whether ubiquitin could bind to AgNP, we performed DMD simulations near room temperature with a ubiquitin molecule initially positioned away from a citrate-coated AgNP (Fig. 1c). Interestingly, we found that the neutrally-charged ubiquitin did not bind to the hydrophobic surface of AgNP, but instead attracted to the surface charge of the AgNP by replacing the surface-bound citrates (-3e at neutral pH) that were stabilized by electrostatic interactions (Fig. 1c). Although ubiquitin does not have a net charge, it does possess eleven positively-charged and eleven negatively-charged residues out of the 76 total residues[23]. Near the surface of the ubiquitin helix, negatively-charged residues formed a cluster with low electrostatic potentials, which allowed stronger binding to the AgNP in simulations than did the negatively-charged citrates.

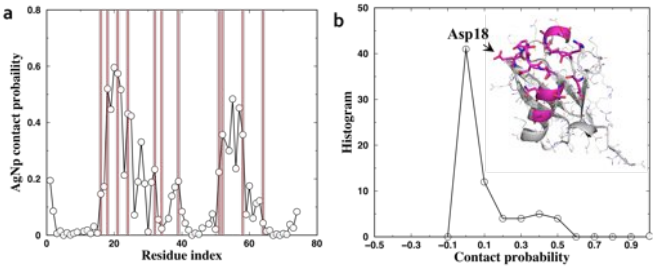


**Figure 2. Specific binding between ubiquitin and AgNP.** (a) The contact probability between AgNP and each ubiquitin residue, computed from all-atom DMD simulations. (b) The histogram of the AgNP-ubiquitin contact probability displays a bimodal distribution. The ubiquitin residues with high contact frequency (> 0.3) to the AgNP are shown in sticks (insert).

Based on the ensemble of ubiquitin-bound complex structures derived from seven independent DMD simulations, we computed for each residue the probability of forming contact with the nanoparticle. Only a subset of residues had significantly high AgNP contact frequency, *PAgNP*, while the rest of the protein did not interact with the AgNP (Fig. 2a). The histogram of *PAgNP* featured a bimodal distribution, with one peak close to zero and the other centered around *PAgNP* ~ 0.4 (Fig. 2b). We further determined the AgNP-binding residues (Fig. 2b insert) as those with *PAgNP* larger than 0.3, the median value separating two peaks in the histogram. These residues were located near the protein helix (Fig. 1d). Although electrostatic interaction was the driving force for AgNP-ubiquitin binding, intriguingly only a fraction of the negatively-charged residues had high contact frequencies with the positively-charged AgNP surface (Fig. 2a). Since these negatively-charged residues are scattered on the surface

of ubiquitin, it was unknown *a priori* where these AgNP-binding residues located. Importantly, one of the AgNP-binding residues, Asp18 (*PAgNP* = 0.52), had been experimentally determined to bind gold nanoparticle (AuNP) by nuclear magnetic resonance (NMR) studies[24]. Since AgNP and AuNP are comparable both physically and chemically, we believe that the modes of their binding with ubiquitin are also comparable. This agreement between NMR observations and simulations highlights the predictive power of our computational methods.

In order to observe the formation of AgNP-ubiquitin corona *in silico*, it is necessary to include multiple proteins in simulations, which is beyond the capacity of atomistic simulations. Instead, we used a two-bead-per-residue model[25] to represent ubiquitin and a single atom to model each citrate. The inter- and intra-ubiquitin interactions were modeled by a structure-based potential model, which has been extensively used in computational studies of protein folding and protein aggregation[21]. The specific interactions between the AgNP surface charges and ubiquitin residues as well as other non-specific inter-molecule interactions were modeled according to atomistic DMD simulations.

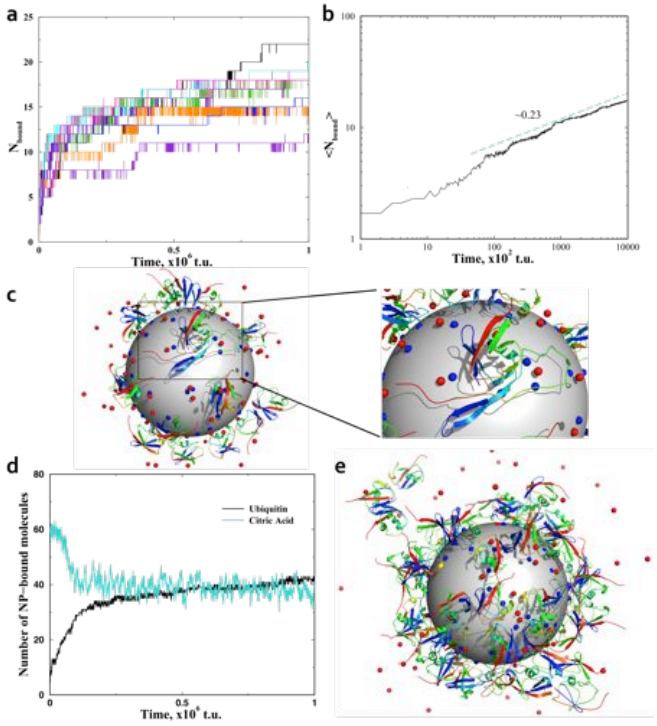


**Figure 3. Ubiquitin-AgNP corona formation.** (a) The number of ubiquitin molecules bound to AgNP, $N_{bound}$, was computed as the function of time from ten independent simulations (in different colors) of the coarse-grained molecular system. (b) The average number of ubiquitins bound to AgNP, $<N_{bound}>$, features a power-law (approximately linear) in a log-log plot. (c) The final structure from one of the simulations. The ubiquitins are in cartoon representation. The citrates correspond to the red spheres. The blue spheres on the surface of the AgNP are the positively charged atoms. One of AgNP-bound ubiquitin is unfolded on the nanoparticle surface (right). In a coarse-grained DMD simulation with a higher stoichiometry of ubiquitin to AgNP (50:1), ubiquitin competed with citrate to bind AgNP by displacing initially-bound citrates (d). At this high stoichiometry, multi layers of ubiquitins were found to deposit onto the surface of the AgNP (e).

We investigated AgNP-ubiquitin corona formation by performing DMD simulations of the coarse-grained system, with multiple ubiquitins (25 molecules) initially positioned randomly with respect to a citrate-coated AgNP. The temperature of the simulation system was kept below the melting temperature of ubiquitin in order to mimic the physiological conditions, where the protein remains folded. To avoid potential biases associated with initial conditions, we performed ten independent simulations assuming different initial configurations and velocities. For each simulation we monitored the number of ubiquitins bound to the AgNP, *Nbound*, as a function of time. All trajectories in Fig. 3a featured an initial fast binding, which slowed down as time progressed. Interestingly, the average *Nbound* did not follow a typical single-exponential binding kinetics, ~ 1-$exp(-\lambda t)$, which usually features a power-law with the exponent of 1 during initial binding in a log-log plot (Fig. 3b). Instead, the exponent is ~0.23 < 1, corresponding to a stretched-exponential binding kinetics, ~ 1-$exp(-ct^{\alpha})$. Similar stretched-exponential binding kinetics has been reported for human serum albumin absorption onto a colloidal nanoparticle. Therefore, our coarse-grained simulations recapitulated the experimentally-observed stretched exponential binding kinetics and revealed the molecular mechanism leading to the complex behavior for nanoparticle-protein binding. Such mechanism may be considered in future kinetic and mesoscopic modeling of corona formation, such as studies of the Vroman effect of abundant proteins for a nanoparticle entering the bloodstream.

The AgNP-ubiquitin complex structure derived from simulations had multiple ubiquitins bound to the surface of one AgNP, forming a single-layer protein corona (Fig. 3c). The majority of AgNP-bound proteins stayed folded under the particular simulation condition and bound to the surface of the AgNP with the protein helix facing the nanoparticle. Only in one of the simulations, one ubiquitin out of the 22 AgNP-bound proteins partially unfolded and the conformation was stabilized by extensive contacts with the hydrophobic surface of the AgNP (Fig. 3c). In addition, we explored the effect of protein concentration on corona formation by performing DMD simulation for a higher ubiquitin/AgNP stoichiometry of 50:1. In these simulations, ubiquitins competed with citrates for binding to the AgNP (Fig. 3d). The final structure featured multiple layers of protein corona, whereas the first layer was dominated by specific binding between ubiquitins and the AgNP, and the outer layers were stabilized by protein-protein interactions (Fig. 3e). This observation is consistent with our dynamic light scattering measurement, where the hydrodynamic size of AgNP-ubiquitin was increased from ~35 nm at AgNP:ubiquitin ratios of 1:100 and 1:500 to 44 nm and 52 nm at AgNP:ubiquitin ratios of 1:1,000 and 1:2,000,

respectively. Thus the AgNP-ubiquitin complex structures derived from the coarse-grained simulations successfully revealed an atomic picture of the nanoparticle-protein corona.

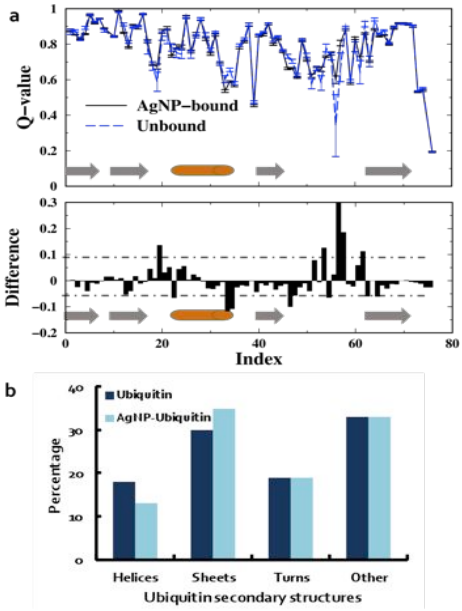


**Figure 4. The structural change of ubiquitin upon AgNP binding.** (a) The fraction of native contacts, Q-value, was computed for each residue for both the AgNP-bound (black) and unbound (blue) ubiquitins (top panel). The differences of Q-value were computed between AgNP-bound and unbound (bottom panel) cases. (b) The percentage of secondary structures in ubiquitin (dark blue) and in AgNP-ubiquitin (cyan) were probed by CD experiments

The ability of nanoparticles to induce protein unfolding (Fig. 3c) could be one of the mechanisms of nanotoxicity. To evaluate the impact of AgNP-binding on ubiquitin conformation, we computed for each protein residue the fraction of native contacts (Q-value) for both the AgNP-bound and unbound ubiquitins (Fig. 4a). A residue with its Q-value close to 1 maintains a native-like structure, while losing its structure if the Q-value is near 0. Both the AgNP-bound and unbound ubiquitins maintained native-like structures with most regions having their Q-values close to 1. Only loop regions between the secondary structures (18-19, 32-35, and 46-53) had relatively low Q-values. The difference in the Q-values for AgNP-bound and unbound ubiquitins suggests that residues in contact with the AgNP were stabilized upon binding (the regions with positive differences coincided with the residues bound to AgNP, Fig. 2a). Two regions, one near the C-terminal of the helix and the other close to residue 46 in a loop, were significantly destabilized upon binding. The destabilization of protein helix due to AgNP-binding is consistent with our circular dichroism (CD) measurement, which revealed that the helical content was reduced by 5% for the AgNP-bound ubiquitins compared to the free ubiquitins (Fig. 4b). The increase of β-sheet content could be due to the formation of inter-protein hydrogen bonds between partially unfolded protein regions, since the protein concentration was locally enriched on the AgNP surface.

## REFERENCES


[1] Lowry, G. V.; Gregory, K. B.; Apte, S. C.; Lead, J. R. *Environ Sci Technol* **2012**, *46*, 6893-9.
[2] Maynard, A. D.; Aitken, R. J.; Butz, T.; Colvin, V.; Donaldson, K.; Oberdorster, G.; Philbert, M. A.; Ryan, J.; Seaton, A.; Stone, V.; Tinkle, S. S.; Tran, L.; Walker, N. J.; Warheit, D. B. *Nature* **2006**, *444*, 267-9.
[3] Schrurs, F.; Lison, D. *Nat Nanotechnol* **2012**, *7*, 546-8.
[4] Cedervall, T.; Lynch, I.; Lindman, S.; Berggard, T.; Thulin, E.; Nilsson, H.; Dawson, K. A.; Linse, S. *Proc Natl Acad Sci U S A* **2007**, *104*, 2050-5.
[5] Nel, A. E.; Madler, L.; Velegol, D.; Xia, T.; Hoek, E. M.; Somasundaran, P.; Klaessig, F.; Castranova, V.; Thompson, M. *Nat Mater* **2009**, *8*, 543-57.
[6] Sund, J.; Alenius, H.; Vippola, M.; Savolainen, K.; Puustinen, A. *Acs Nano* **2011**, *5*, 4300-4309.
[7] Ge, C.; Du, J.; Zhao, L.; Wang, L.; Liu, Y.; Li, D.; Yang, Y.; Zhou, R.; Zhao, Y.; Chai, Z.; Chen, C. *Proc Natl Acad Sci U S A* **2011**, *108*, 16968-73.
[8] Zuo, G.; Huang, Q.; Wei, G.; Zhou, R.; Fang, H. *ACS Nano* **2010**, *4*, 7508-14.
[9] Ratnikova, T. A.; Govindan, P. N.; Salonen, E.; Ke, P. C. *ACS Nano* **2011**, *5*, 6306-14.
[10] Shang, J.; Ratnikova, T. A.; Anttalainen, S.; Salonen, E.; Ke, P. C.; Knap, H. T. *Nanotechnology* **2009**, *20*, 415101.
[11] Shen, J. W.; Wu, T.; Wang, Q.; Kang, Y. *Biomaterials* **2008**, *29*, 3847-55.
[12] Kubiak, K.; Mulheran, P. A. *J Phys Chem B* **2009**, *113*, 12189-200.
[13] Makarucha, A. J.; Todorova, N.; Yarovsky, I. *Eur Biophys J* **2011**, *40*, 103-15.
[14] Marrink, S. J.; de Vries, A. H.; Mark, A. E. *Journal of Physical Chemistry B* **2004**, *108*, 750-760.
[15] Chiu, C. C.; Dieckmann, G. R.; Nielsen, S. O. *J Phys Chem B* **2008**, *112*, 16326-33.
[16] Chiu, C. C.; Dieckmann, G. R.; Nielsen, S. O. *Biopolymers* **2009**, *92*, 156-63.
[17] Hung, A.; Mwenifumbo, S.; Mager, M.; Kuna, J. J.; Stellacci, F.; Yarovsky, I.; Stevens, M. M. *J Am Chem Soc* **2011**, *133*, 1438-50.
[18] Auer, S.; Trovato, A.; Vendruscolo, M. *PLoS Comput Biol* **2009**, *5*, e1000458.
[19] Ding, F.; Dokholyan, N. V. *Trends Biotechnol* **2005**, *23*, 450-5.
[20] Ding, F.; Guo, W.; Dokholyan, N. V.; Shakhnovich, E. I.; Shea, J. E. *J Mol Biol* **2005**, *350*, 1035-50.
[21] Ding, F.; Furukawa, Y.; Nukina, N.; Dokholyan, N. V. *J Mol Biol* **2012**, *421*, 548-60.
[22] Ding, F.; Dokholyan, N. V. *PLoS Comput Biol* **2006**, *2*, e85.
[23] Vijay-Kumar, S.; Bugg, C. E.; Cook, W. J. *J Mol Biol* **1987**, *194*, 531-44.
[24] Calzolai, L.; Franchini, F.; Gilliland, D.; Rossi, F. *Nano Lett* **2010**, *10*, 3101-5.
[25] Ding, F.; Dokholyan, N. V.; Buldyrev, S. V.; Stanley, H. E.; Shakhnovich, E. I. *Biophys J* **2002**, *83*, 3525-32.